Journal of Applied Polymer Science

The Index of Dry-Jet Wet Spinning for Polyacrylonitrile Precursor Fibers

Tai-Yuan Wang,[1] Hsiao-Chuan Chang,[2] Yu-Tsung Chiu,[2] Jia-Lin Tsai[1]

[1]Department of Mechanical Engineering, National Chiao Tung University, Hsinchu, Taiwan

[2]Department of Multiscale Simulation, Material and Chemical Research Laboratories, Industrial Technology Research Institute, Chutung, Hsinchu, Taiwan

Correspondence to: Y.-T. Chiu (E-mail: yutschiu@itri.org.tw)

ABSTRACT: A new spinning index for a PAN precursor fiber is proposed that includes the viscosity of a spinning dope, the thermodynamic affinity, and the draw ratio during the spinning process. Through dry-jet wet spinning, six types of PAN precursor fibers with different spinning parameters, including solid content, solvent content in a bath, and draw ratio, were fabricated and analyzed with tensile tests, SEM, and XRD. The results show that the spinning index can reflect the mechanical properties of the fibers but is less indicative of crystallinity. Hence, the current spinning index is recommended for use as an indicator for the mechanical properties of PAN precursor fibers. © 2014 Wiley Periodicals, Inc. J. Appl. Polym. Sci. **2015**, *132*, 41265.

KEYWORDS: fibers; phase behavior; viscosity and viscoelasticity

Received 8 April 2014; accepted 29 June 2014

DOI: 10.1002/app.41265

INTRODUCTION

Carbon fibers have been extensively used as reinforcements in composites because they have excellent mechanical properties as reinforcements. Nearly 90% of the carbon fiber in the world is made from polyacrylonitrile precursor. The heredity of the structure and the properties of the polyacrylonitrile precursor fiber will affect the subsequent carbon fiber properties through oxidation and carbonization[1,2]; many studies have focused on how to improve the properties of polyacrylonitrile precursor fibers by controlling the manufacturing process. Because the melting temperature of most polyacrylonitriles is higher than their pyrolysis temperature of 317°C, melt-spinning is not suitable for fiber production. In addition, electron-spinning has high cost, low output, and poor properties; hence, solution spinning is generally chosen to fabricate massive polyacrylonitrile fibers.[1] Solution spinning can be divided into dry spinning and wet spinning. In dry spinning, PAN spinning dope is extruded through a dryer can and coagulates with the evaporation of solvent. Because of the low draw ratio and the difficulty of controlling the solvent content, a precursor fiber with the required properties for carbon fibers is hard to be produced through dry spinning. Hence, the PAN precursor fibers are mainly fabricated through wet spinning.[3,4] Wet spinning includes normal wet spinning and dry-jet wet spinning. The difference between these two processes is that when the spinning dope is extruded from the spinneret, there is an air gap in dry-jet wet spinning to relax the stress and allow the solvent to diffuse outward. Then, the solution enters a coagulation bath and experiences phase separation. Therefore, dry-jet wet spinning can reduce the fiber voids and surface collapse due to coagulation and also generates fibers with smoother surfaces and better mechanical properties.[4] Fibers generated via dry-jet wet spinning were used in the current study.

In addition to the aforementioned differences between the spinning methods, the properties of the precursor fibers are also influenced by the fabrication of the spinning dope and the spinning processes. Some important factors that have been studied include spinning dope,[5–7] spinning parameters and conditions,[8–10] and additions.[11–13] First, with respect to the spinning dope, Hou et al.[5] studied the influence of H_2O/DMSO mixture suspension polymerization, aqueous suspension polymerization, and DMSO solution polymerization on the phase separation of PAN fibers under the same coagulation conditions. Their results showed that the fibers obtained through aqueous solution polymerization have gentler exchange behavior between solvent and non-solvent and higher crystallinity. Yin et al.[6] also demonstrated that aqueous suspension polymerization can be used to obtain fibers with round cross-sections. By increasing the solid content of the copolymer in the dope, the diffusion between solvent and non-solvent can be mitigated in the coagulation bath. Arbab et al.[7] showed that PAN fibers made from dope with a higher solid content had a lower porosity, a smaller pore size, and greater tensile strength.

In the spinning process, scholars were interested in various influences of the spinning parameters, including the diameter and number of spinneret holes, the length of the air gap, the composition and temperature of the coagulation bath, the draw ratio during water washing, and the hot drawing and steam drawing processes. Bajaj et al.[8] found that increasing the temperature of the coagulation bath would lead to an increase in the fiber diameter and a decrease in the fiber density. Their results showed that the draw ratio only influences the crystal size and orientation but does not affect the crystallinity. Peng et al.[9] investigated the effect of the solvent content in the coagulation bath on the structure and properties of nascent PAN fibers. Their results showed that when the DMSO content increases from 43 to 70 wt %, the consequent fibers have higher crystallinity and crystal size with round cross-sections. However, if the DMSO content continues to increase, the diffusion of the solvent will become too slow, leading to precursor fibers with surface collapse and worse mechanical properties. Zhang et al.[10] discussed the influence of the solvent type on the nascent fibers. The composition of ethanol/DMSO/PAN had a higher miscibility gap than water/DMSO/PAN. The phase separation of the spinning dope occurring in the meta-stable two-phase region could make the fibers denser and could improve the mechanical properties.

The properties of PAN precursor fibers are influenced by many factors in the spinning process; hence, how to estimate the structure and properties with certain spinning parameters is an issue in fiber fabrication. Ruaan et al.[14] proposed a simple index with the basic concept of the time needed for phase separation completion, and they used it as a selection criterion for film wet phase inversion. Two major factors of the phase separation time are the precipitant volume and the exchange rate between solvent and non-solvent. When the exchange rate is fixed, the system with the smallest precipitant volume has the shortest separation time; hence, the phase separation behavior is deeply affected by interactions between the solvent and non-solvent, the solvent and polymer, and the non-solvent and polymer. By considering the effect of the interactions of the solvent and non-solvent on the miscibility gap, Hansen solubility parameters are used to measure the interactions in the solvent/non-solvent/polymer system. After verification with many systems with different compositions, their index could approximately divide the morphology of films into two types. If the phase separation is gentle, the index is smaller, and the corresponding film is sponge-like with smaller voids. On the contrary, if the phase separation is strong, then the index is large, and the corresponding film has large finger-like voids. Arbab et al.[15] followed the spirit of the aforementioned research to estimate the fiber porosity with the Hansen solubility and viscosity of the spinning dope. According to their results, the dope with a higher solid content had higher viscosity and a smaller index, and the follow-up precursor fiber had smaller porosity and better mechanical properties.

From the above reviews, we can see that different spinning parameters influence the micro-structure and properties of the precursor fiber. Some researchers have tried to investigate the index of films or wet spinning fibers using the solubility parameters and viscosity. However, that research, which focuses on the correlation between the mechanical properties of fibers through dry-jet wet spinning and certain spinning parameters, is still limited.

To estimate properties of precursor fibers before actual spinning process, the spinning index would be a meaningful reference for the sequence oxidation fibers as well as carbon fibers. Hence, the existed forms of index, that have been proposed by forerunners were adopted and further developed by introducing the draw ratio in current study. In addition, we analyze the effect of the solvent content in the bath, the total draw ratio, and the solid content of the spinning dope on the mechanical properties of dry-jet wet spinning fibers to validate the applicability of current spinning index.

EXPERIMENTAL

Construction of the Spinning Index

Making better quality PAN precursor fibers is a persistent goal of carbon fiber manufacturing. Hence, in this study, we want to propose some key parameters of the spinning index from factors that are already known to influence fiber properties. In the work presented by Arbab et al.,[15] the index was composed of the thermodynamic affinity calculated by the square difference of the Hansen solubility parameters and the on-line viscosity.[16] They connected their index with the porosity of the fibers and then used porosity-dependent equations to link the mechanical properties. In the current study, the above factors are also considered to be important factors that are confirmed to influence both the fiber structure and the mechanical properties of the fibers. In addition, we further considered the draw ratio during the spinning process, which has been reported to be an important parameter of the mechanical properties.[8] Some results from the available literature were collected and exhibited the effect of the viscosity of the dope, the phase separation behavior (which could be controlled by changing the solvent content in the bath), and the draw ratio for constructing the spinning index.

Viscosity. In the process of fiber spinning, the viscosity of spinning dope is an important index for the rheology properties as well as entanglements for polymer chains. In the viewpoint of Arbab et al.,[7,11] the higher viscosity may be treated as the rheological barrier for phase separation which tenders the exchange between solvent and nonsolvent. The dope with higher polymer concentration exhibits higher viscosity as well as lower overall porosity for resulting fibers.

In our viewpoint, the spinning dope with higher viscosity may represent the higher entanglement and network for polymer chains, which is supported by the fact the mechanical properties of as-spun fibers are highly positive related to the entanglement degree.[17]

Tsai and Lin discussed the effect of the PAN molecular weight on the mechanical properties of precursor fibers through wet spinning.[18] The relation between the viscosity, tensile strength and fiber orientation are shown in Figure 1. Although their dope had a low viscosity (within the range of 2000cps to 4250cps), it still exhibited a nearly positive relation in both tensile strength and orientation. In the current research, the

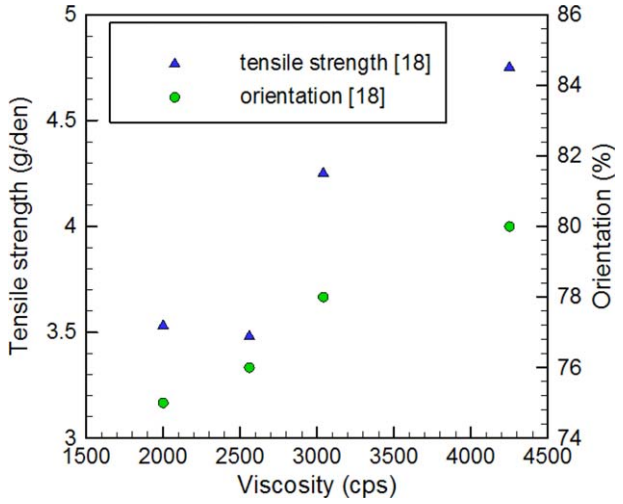

Figure 1. The effect of the viscosity of the spinning dope on the tenacity and orientation of the PAN precursor fibers; all data are extracted from Ref. 18. [Color figure can be viewed in the online issue, which is available at wileyonlinelibrary.com.]

dynamic shear viscosity of the spinning dope was measured to estimate the polymer state in the dope tank. To obtain the dimensionless viscosity η for the spinning index calculation, the measured dynamic viscosity at the same temperature as the extruding temperature (60°C) was divided by 10^6 cps and treated as a numerator in the spinning index.

Phase Separation. The phase separation of the spinning dope in the coagulation bath was reported to be an important factor that significantly influences the properties of the precursor fibers.[9,10] The primary microstructures of the fibers are determined when the spinning dope encounters the coagulation bath, as shown in Figure 2. According to Flory–Huggins theory,[19] the interaction parameters of two arbitrary components in the polymer/solvent/non-solvent system are in direct proportion to the square difference of their solubility parameters. Furthermore, the meta-stable region for demixing mechanism of nucleation and growth (NG) is influenced by the interaction parameters.[10] The phase separation of the spinning system with a smaller meta-stable region likely undergoes spinodal decomposition and results in fibers with loose structures.[10,20] To measure the behavior of the phase separation, we followed the procedure of Ruaan et al.[14] to define the dimensionless thermodynamic affinity as

$$\Phi \equiv \frac{\Delta\delta^{p-s}\Delta\delta^{p-ns}}{\delta_t^p \Delta\delta^{s-ns}} \tag{1}$$

$$\Delta\delta^{i-j} = \left[\left(\delta_d^i - \delta_d^j\right)^2 + \left(\delta_p^i - \delta_p^j\right)^2 + \left(\delta_h^i - \delta_h^j\right)^2\right]^{\frac{1}{2}} \tag{2}$$

where $\Delta\delta^{p-s}$, $\Delta\delta^{p-ns}$, and $\Delta\delta^{s-ns}$ correspond to the difference of the Hansen solubility between the polymer and solvent, the polymer and nonsolvent, and the solvent and non-solvent, respectively; and δ_t^p is the total Hansen solubility parameter of the polymer.[16] The symbol δ in eq. (2) represents Hansen solubility parameter, where the superscripts i and j represent the component in the polymer/solvent/non-solvent system; the subscripts *d*, *p*, and *h* represent the solubility parameters contributed by van der Waals forces, polarity and hydrogen bonds, respectively. The Hansen solubility parameters used in the current study are listed in Table I. A simple linear modification of the weight fraction is used if any solvent is added in the coagulation bath or if non-solvent is added into the spinning dope.[14] To connect the phase separation with the mechanical properties of the fibers, thermodynamic affinity Φ was treated as a denominator in the spinning index. Wang et al.[21] investigated the effect of the DMSO content in the bath on the fiber tenacity through wet spinning. Based on eq. (2) and a certain solvent content, the relation between the corresponding Φ^{-1} and the fiber tenacity is plotted in Figure 3 as a positive relation. The concentrations of solvent in the bath were 30, 40, 50, 60, and 70 wt %, which correspond to the five points from left to right in the plot. The tenacity increases when the solvent content is <50 wt %. Then, the growth becomes slight with higher solvent concentrations. Zhou et al.[22] investigated the influence of the solvent content on nascent PAN fibers. In their results, the cross-section of the nascent fibers with 60 wt % DMSO in the bath was uniform and denser than those with 50 wt % DMSO in the bath. In addition, the corresponding Φ^{-1} values were 11.58 and 9.83, respectively, for cases with 60 and 50 wt % DMSO in the bath, indicating that the reciprocal of the thermodynamic affinity has the ability to reflect both the fiber properties and the structure.

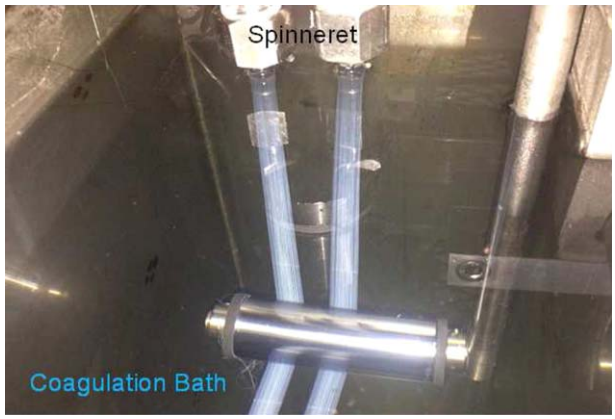

Figure 2. Photos of the fiber formation by encountering nonsolvent during the coagulation bath. [Color figure can be viewed in the online issue, which is available at wileyonlinelibrary.com.]

Draw Ratio. In the dry-jet wet spinning process, polymer chains in each fiber experience uniaxial tension as drawing stress. Meanwhile, polymer chains become oriented gradually.[23]

Table I. Hansen Solubility Parameters Used in the Current Study[16]

System		Solubility parameter δ [(J cm^{-3})$^{1/2}$]			
		δ_d	δ_p	δ_h	δ_t
Polymer	PAN	21.7	14.1	9.1	27.4
Solvent	DMSO	18.4	16.4	10.2	26.7
Non-solvent	water	15.5	16	42.3	47.8

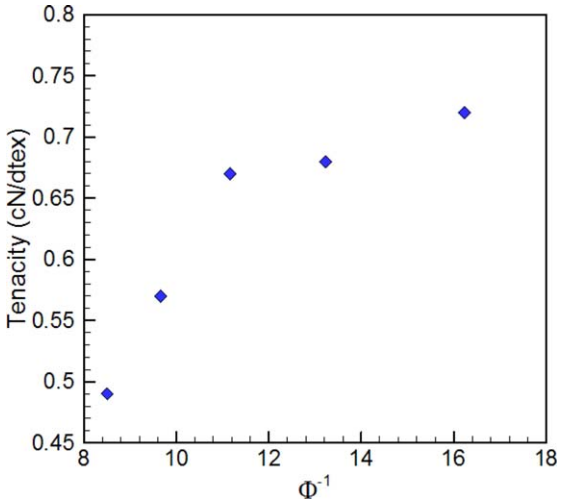

Figure 3. The effect of the thermodynamic affinity on the tenacity and orientation of the PAN precursor fibers, all data are extracted from Ref. 21. [Color figure can be viewed in the online issue, which is available at wileyonlinelibrary.com.]

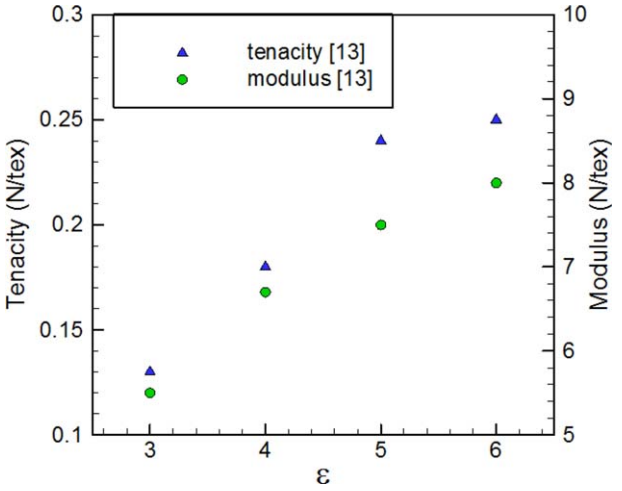

Figure 5. The effect of the total draw ratio on the tenacity and modulus of the PAN precursor fibers; all data are extracted from Ref. 13. [Color figure can be viewed in the online issue, which is available at wileyonlinelibrary.com.]

Moreover, some scholars discovered the influence of the draw ratio on the mechanical properties of the polymer fibers.[8,24–26] In the work done by Yu et al.,[25] a fact that the optimization of draw ratio is necessary to obtain the best quality of fibers has been exhibited. Hence the attempts of correlating the draw ratio and mechanical properties should be meaningful to industrial application as well as theory investigation.

Bajaj et al.[8] showed a positive relation between the draw ratio ε and the mechanical properties of the PAN precursor fibers, as shown in Figure 4. In addition, Jain et al.[13] showed a similar trend for PAN fibers, as seen in Figure 5. In the current study, the draw ratio was defined as the ratio of the speed of the wind-up drum to the speed of the first roller after the coagulation bath. To consider the influence on the polymer morphology, the draw ratio was treated as a numerator in the spinning index.

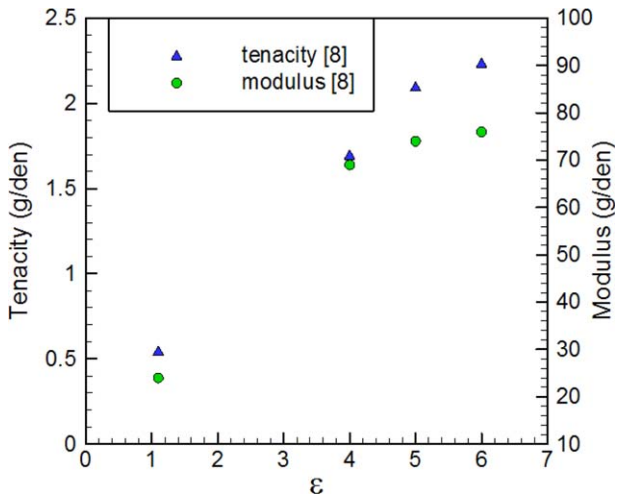

Figure 4. The effect of the total draw ratio on the tenacity and modulus of the PAN precursor fibers; all data are extracted from Ref. 8. [Color figure can be viewed in the online issue, which is available at wileyonlinelibrary.com.]

Spinning Index. By considering all relations between the spinning parameters and the mechanical properties above and for the convenience of estimating the spinning quality of fiber fabrication, a spinning index S is primary defined as

$$S \equiv \frac{\eta\varepsilon}{\Phi} \tag{3}$$

where η is the normalized viscosity of the spinning dope, Φ is the index of phase separation, thermodynamic affinity, and ε is total draw ratio in the spinning process. To perform qualitative estimation, the temperature effect on the phase separation during the coagulation bath and the spinnability are not considered in the current spinning index.

Fabrication of PAN Precursor Fibers

In the current study, the spinning dope was composed of acrylonitrile monomers and 2 wt % itaconic acid to form PAN-IA copolymers with an intrinsic viscosity of 1.89 dL g^{-1}. The solvent, dimethyl sulfoxide, was purchased from ECHO Chemical. To discuss the influence of the viscosity of the spinning dope on the structure and properties of the precursor fibers, spinning dopes with solid contents of 20 and 21 wt % were prepared at 70°C and then kept at 60°C in the dope reservoir. Dry-jet wet spinning was used to fabricate PAN precursor fibers with a platinum dual-spinneret that had 300 holes with diameters of 80 μm, as shown in Figure 2. The air gap in the current study was chosen to be 0.5 cm. During the spinning process, fibers passed four troughs, a coagulation bath, a pre-extension bath, an extension bath, and a water bath in sequence. The volume ratio between DMSO and water in the coagulation bath was designed as 0 : 100, 5 : 95, and 10 : 90 to investigate how the concentration of the solvent in the coagulation bath influences the fiber properties. Additionally, pure water was used in the other baths. The temperatures of the coagulation bath, pre-extension bath, extension bath, water bath, drying, and steam drawing were

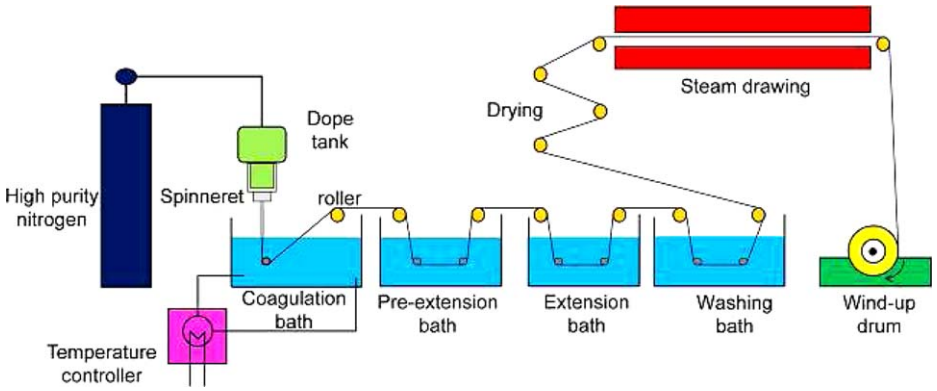

Figure 6. Sketch of the current dry-jet wet spinning line. [Color figure can be viewed in the online issue, which is available at wileyonlinelibrary.com.]

kept at 10, 60, 70, 80, 120, and 140°C, respectively. The total draw ratio was set as 7.5, 8.5, and 9.5 to explore the effect of the draw ratio. The spinning line of the current study is illustrated as Figure 6. The nomenclature of the six samples of PAN precursor fibers with different spinning parameters is listed in Table II.

Characterization of PAN Fibers

As shown from the literature in the introduction, there are plenty of analyses to study the relation between the mechanical properties and the structure of fibers, including XRD, SAXS, DSC, TGA, and porosity. Hence, the current research mainly targeted the construction of a correlation between the influential spinning parameters and the mechanical properties of fibers. The characterization of PAN fibers focused on the cross-section morphology, linear density, mechanical properties, and crystallinity. To calculate the spinning index *S*, the viscosity of the spinning dope was also measured by a Brookfield viscometer at 50, 60, and 70°C within the ranges of the extruding temperature. In addition, to understand the influence of the solvent content in the bath and the draw ratio on the fiber microstructure, high-resolution scanning electron microscopy was used to observe the morphology of the fiber cross-sections. A tensile test of the single precursor fiber was performed with a ZWICK 1445 with a 5N load cell, a gauge length of 25 mm, a crosshead speed of 10 mm min^{-1}, and sample numbers 15–20. During the tensile tests, the engineering stress and strain were calculated as the force and displacement divided by the initial cross-section of the fiber. The linear density of the fibers was measured by weighing an individual fiber with a length of 90 cm.

The crystalline state was measured using a PW3040 X-ray diffractometer with a Cu target, a voltage of 45 kV, and a current of 40 mA. The scan angle ranged from 10° to 40° in 0.04° steps. To calculate the crystallinity C, there are many methods to decide the proper integrated area for a crystal in a diffractogram.[27–29] In the current study, the method used in the literature[27] was applied to define the crystallinity as

$$C = \frac{A_C}{A_T} \times 100\% \quad (4)$$

where A_C is the integrated area of the crystalline domain of the PAN fibers at $2\theta = 16.8°$, and A_T is the total integrated area. The crystal size L_C and *d*-spacing were calculated using the Scherrer equation and Bragg's law, respectively.

Table II. Sample Nomenclature and Spinning Conditions

Sample	Solid content (wt %)	Coagulation bath composition	Total drawing ratio
P1	21	0% DMSO+100% water	9.5
P2	21	5% DMSO+95% water	9.5
P3	21	10% DMSO+90% water	9.5
P4	20	10% DMSO+90% water	7.5
P5	20	10% DMSO+90% water	8.5
P6	20	10% DMSO+90% water	9.5

RESULTS AND DISCUSSION

Morphology and Properties of PAN Precursor Fibers

Figure 7 shows the comparison of the viscosity of the solid content 20 and 21 wt % of PAN doped at three different temperatures. The viscosity of the dope with 21 wt % PAN was higher

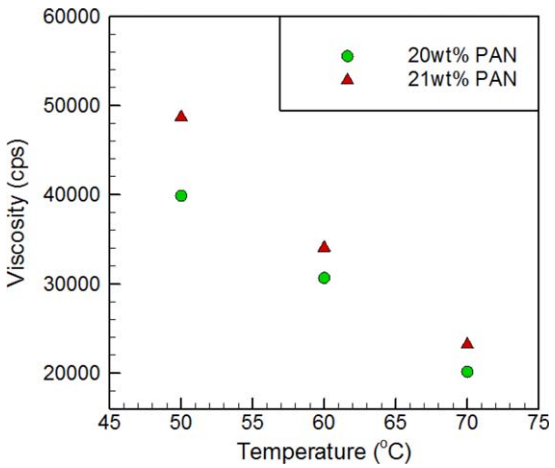

Figure 7. Viscosity of the PAN spinning dope with different solid contents at different temperatures. [Color figure can be viewed in the online issue, which is available at wileyonlinelibrary.com.]

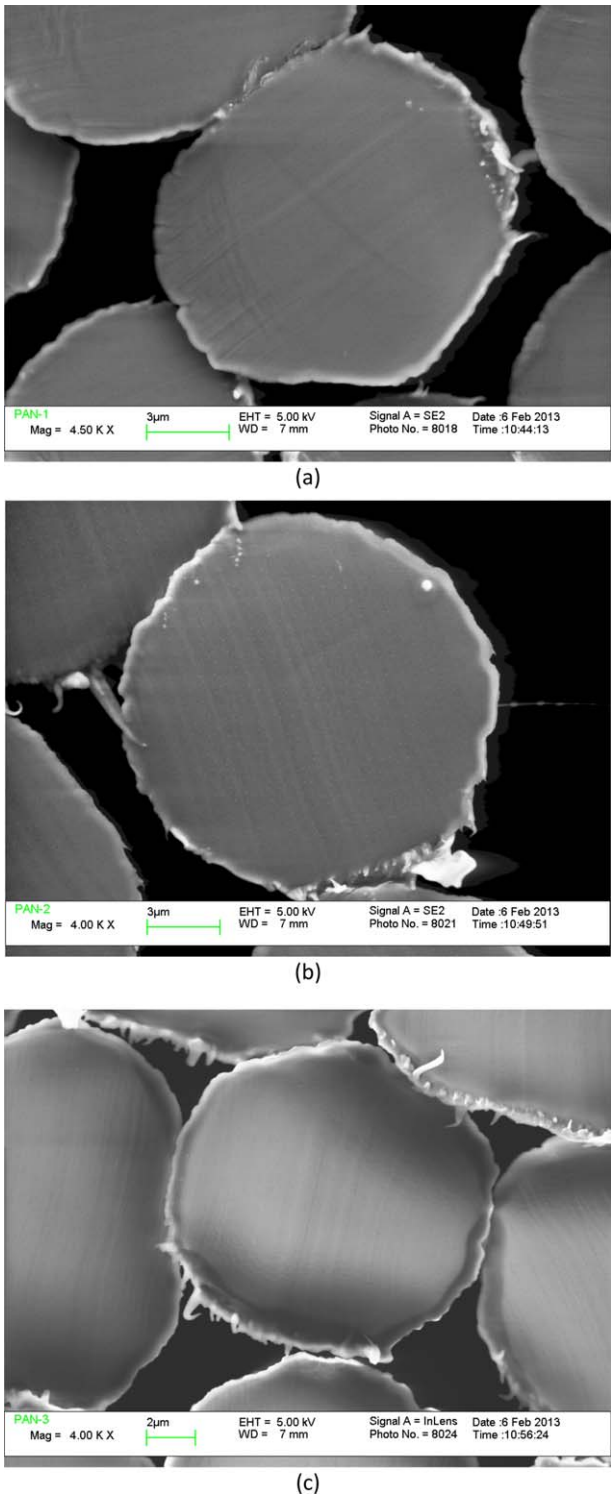

Figure 8. Cross-section photos of the PAN precursor fibers with different solvent contents in the bath, (a) P1-0%, (b) P2–5%, (c) P3–10%. [Color figure can be viewed in the online issue, which is available at wileyonlinelibrary.com.]

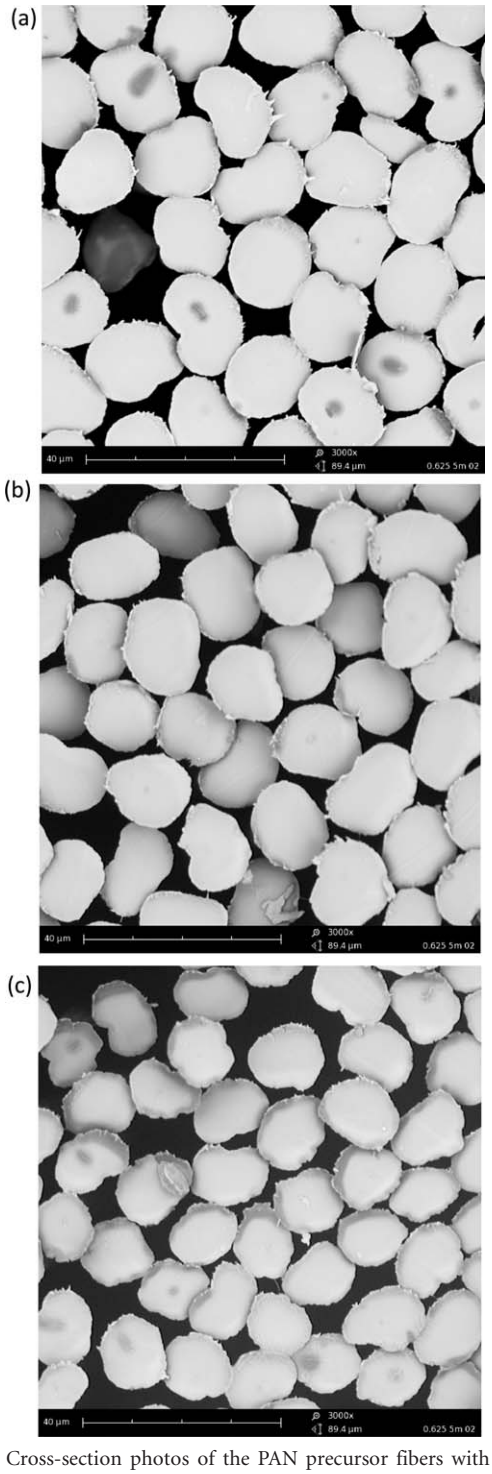

Figure 9. Cross-section photos of the PAN precursor fibers with different draw ratios, (a) P4–7.5, (b) P5–8.5, (c) P6–9.5.

than that with 20 wt % at every temperature. In addition, the viscosity dropped rapidly as the temperature increased, which is consistent with the literature.[8] The cross-section of the PAN precursor fibers in a dope with a high solid content are shown in Figure 8. With the current spinning settings, there are no obvious voids or skin-core structures in Figure 8(a–c). The slight change in the solvent content in the bath did not influence the cross-section; most of the fibers have a round shape. Figure 9 shows the cross-sections of the PAN precursor fibers with draw ratios of 7.5, 8.5, and 9.5. Some fibers with bean-

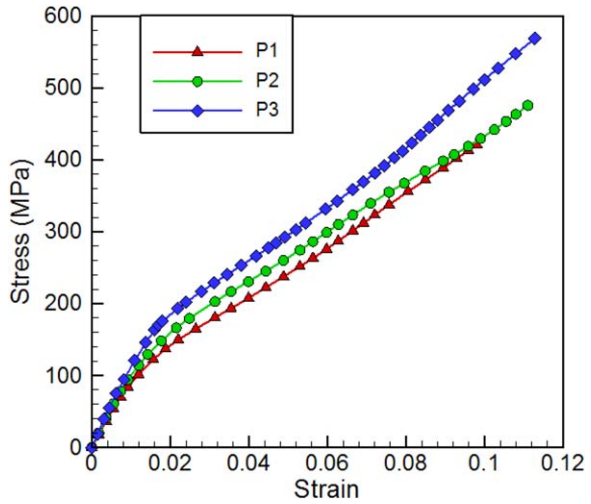

Figure 10. Stress–strain diagram of PAN precursor fibers P1-P3. [Color figure can be viewed in the online issue, which is available at wileyonlinelibrary.com.]

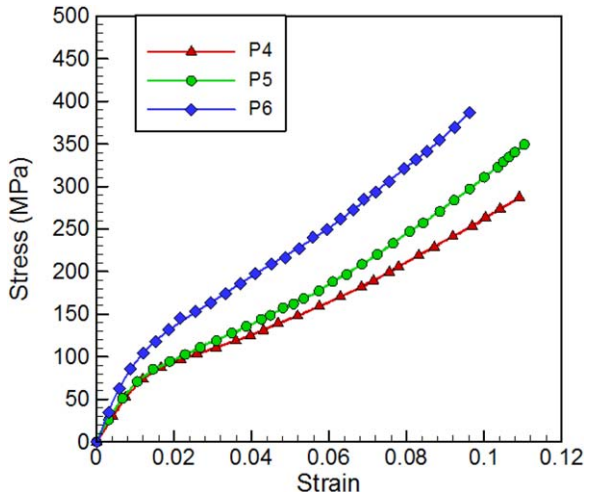

Figure 11. Stress–strain diagram of PAN precursor fibers P4-P6. [Color figure can be viewed in the online issue, which is available at wileyonlinelibrary.com.]

shaped or kidney-shaped cross-sections were observed, and the diameter of the fibers decreased as the draw ratio increased.

In the tensile tests, two series of typical stress-strain curves of PAN precursor fibers were observed, as shown in Figures 10 and 11. The curves grow linearly at first, and then yield at a strain of 0.01. After the yielding point, the curves still grow moderately until breakage occurs. The average mechanical properties of PAN precursor fibers with associated standard errors are listed in Table III. When the draw ratio is fixed, the modulus and the strength of the PAN fibers with higher solid contents increase with the increased solvent content in the bath. As the solvent content increased from 0 to 5 wt %, the tensile modulus increase from 10.89 to 11.77 GPa, the tensile strength increased from 426.94 to 473.25 MPa, and the fracture strain increased from 0.093 to 0.111. When the solvent content further increased to 10 wt %, the tensile modulus and strength exceed 13.79 GPa and 591.87 MPa, respectively, and the fracture strain remains unchanged. The aforementioned trend is consistent with the literature.[21] The main reason for the enhancement of mechanical properties is that the phase separation between PAN, DMSO, and water becomes greater and decreases the nano-size voids in the fibers. Although the cross-section of the P1-P3 fibers does not show the difference directly, the increased linear density supports this point. For low-solid-content fibers (P4-P6) with fixed solvent contents in the bath, the higher draw ratio results in fibers with better mechanical properties. When the draw ratio increased from 7.5 to 8.5, the modulus increased from 7.22 to 8.95 GPa, and the strength increased from 292.33 to 365.31 MPa. After further increasing the draw ratio to 9.5, the modulus and strength exceeded 9.84 GPa and 381.59 MPa, respectively. Additionally, the influence of the draw ratio does not show an obvious trend on the fracture strain, which is in the range of 0.108–0.118.

The relation between the draw ratio and the mechanical properties is consistent with the literature.[8,24–26] However, the enhancement by increasing the draw ratio from 8.5 to 9.5 is less than that achieved by increasing the draw ratio from 7.5 to 8.5. This result indicates that changes in the polymer orientation,[8] size and distribution of voids[26] through drawing have limitations.

When the solvent content in the bath and the draw ratio are fixed, the experimental results show that fibers with a higher viscosity and a high solid content (P3) have better mechanical properties than those with a lower viscosity (P6). This influence is much stronger than the solvent content and the draw ratio, which is consistent with the literature.[7] By comparing the linear densities of these fibers, the reason for the improvement of the mechanical properties may be the reduction of the overall porosity.

Table III. Mechanical Properties of the PAN Precursor Fibers

Sample	Tensile strength (MPa)	Modulus (GPa)	Fracture strain	Linear density (denier)
P1	426.94 ± 97.93	10.44 ± 2.57	0.093 ± 0.02	1.01 ± 0.01
P2	473.26 ± 51.35	11.77 ± 2.27	0.111 ± 0.02	1.31 ± 0.02
P3	591.79 ± 41.18	13.79 ± 1.89	0.118 ± 0.02	1.36 ± 0.02
P4	292.33 ± 21.35	7.22 ± 0.89	0.118 ± 0.01	1.75 ± 0.14
P5	365.31 ± 18.34	8.95 ± 0.94	0.108 ± 0.01	1.50 ± 0.01
P6	381.59 ± 59.71	9.84 ± 1.00	0.118 ± 0.02	1.15 ± 0.20

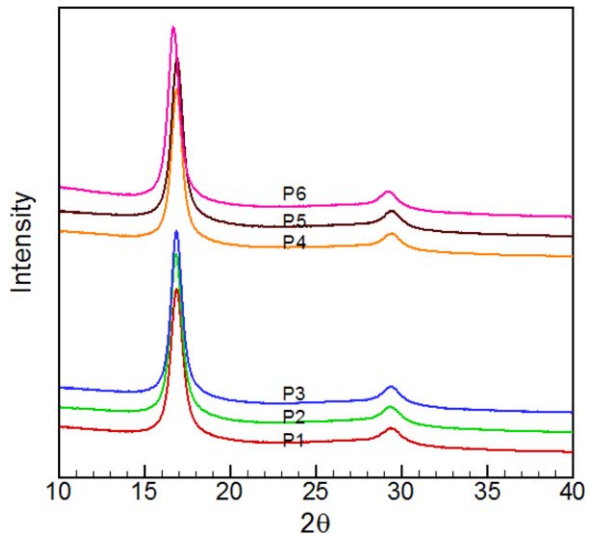

Figure 12. X-ray diffraction patterns of the PAN fibers. [Color figure can be viewed in the online issue, which is available at wileyonlinelibrary.com.]

The XRD patterns are shown in Figure 12, and the corresponding results are listed in Table IV. The current fibers have clear peaks at $2\theta = 16.8°$, which is consistent with the literature.[7,23,25] The curves are similar to the result obtained for a highly drawn PAN film.[30] Essentially, the crystallinity increases gradually with the solvent content in the bath from 26.2 to 27.9% for P1-P3 fibers. The crystal size also increases gradually with the solvent content in the bath from 1.67 to 1.81 nm. The D-spacing at $2\theta = 16.8°$ varied only slightly at ~5.25 Å. The above trend in the crystallinity is the same as both that reported in the literature[9] and that reported in the current study with a low solvent content in the bath.

For P4-P6 fibers, the crystallinity also gradually increases from 26.1 to 27%, the crystal size decreases from 1.85 to 1.78 nm, and the *d*-space at $2\theta = 16.8°$ varies within the range 5.24–5.31 Å. This trend, i.e., crystallinity increasing with the draw ratio, is consistent with the literature[24,25]; however, it is not obvious when comparing to the effect of the solvent content in the bath for the current study. A different view reported in the literature[8] claimed that crystallinity is not affected by the draw ratio. These observations indicate that the effect of the draw ratios on the inner structure may require further discussion, including consideration of applying temperature or the properties of the spinning dope.

Table IV. Degree of Crystallinity, Crystal Size, and *d*-Spacing of the PAN Precursor Fibers

Sample	Crystallinity C (%)	Crystal size L_C (nm)	*d*-spacing (Å)
P1	26.2	1.67	5.25
P2	27.2	1.74	5.26
P3	27.9	1.81	5.25
P4	26.1	1.85	5.24
P5	26.9	1.75	5.24
P6	27.0	1.78	5.30

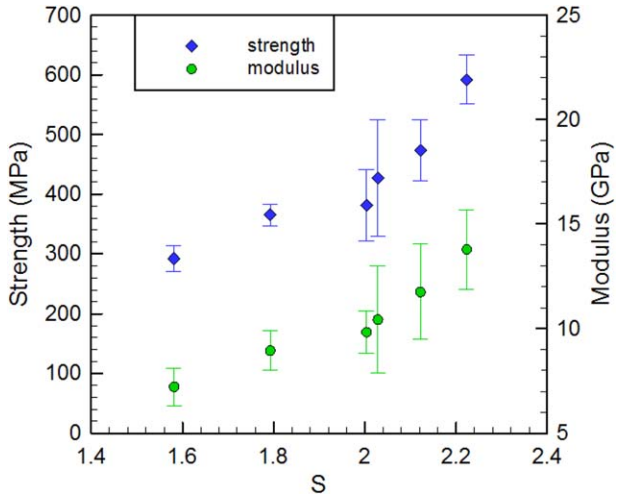

Figure 13. Relation between the mechanical properties and the spinning index *S*. [Color figure can be viewed in the online issue, which is available at wileyonlinelibrary.com.]

Correlation Between Spinning Index and Fiber Properties

In the current study, six PAN fiber samples with two different solid contents, three draw ratios, and three solvent contents in the bath were fabricated. Besides, the corresponding spinning index composed by viscosity, thermodynamic affinity and draw ratio were calculated before the spinning process as Table V. After the analysis of the mechanical properties and the crystalline state, the correlation between the spinning index S and the fiber properties can be obtained, as shown in Figures 13 and 14.

In Figure 13, we can see the ability of the current spinning index *S*, which reflects the mechanical properties well. Even the mechanism of the modulus improvement and strength improvement is usually different in mechanics. The correlation between the modulus and *S* shows a similar trend with the correlation

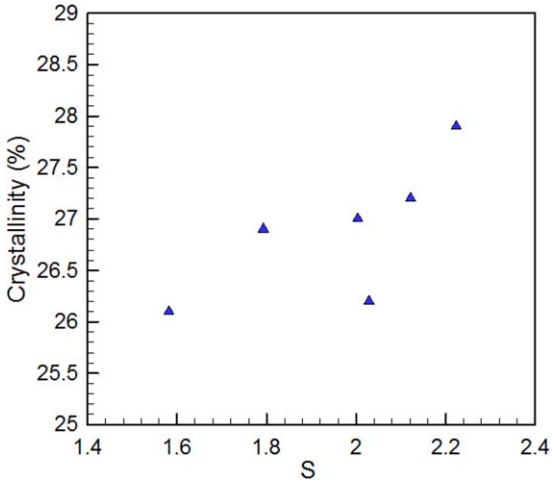

Figure 14. Relation between the crystallinity and the spinning index *S*. [Color figure can be viewed in the online issue, which is available at wileyonlinelibrary.com.]

Table V. Spinning Index and Ingredient Parameters of PAN Precursor Fibers

Sample	η	Φ^{-1}	ε	S
P1	0.034066	6.268186	9.5	2.0285
P2	0.034066	6.555557	9.5	2.1215
P3	0.034066	6.870543	9.5	2.2234
P4	0.030696	6.870543	7.5	1.5817
P5	0.030696	6.870543	8.5	1.7926
P6	0.030696	6.870543	9.5	2.0035

between the strength and *S*. This result indicates that for fiber material prepared through dry-jet wet spinning, the viscosity of the dope, the thermodynamics affinity, and the draw ratio might have the same effect on the fiber modulus and strength, which is worthy of deeper discussion. The error bars in the figure, which represent the standard deviation for the corresponding sample, also show an interesting trend with index *S*. For both the modulus and the strength, samples with higher *S*, which have higher η and three levels of Φ^{-1}, also have larger coefficients of variation (defined as the standard deviation divided by the average). This trend indicates that the increasing solid content or decreasing solvent content in the bath may accompany the differentiation of the fiber structure during spinning. The fact that the draw ratio influences the fiber properties, as shown in the literature, is confirmed,[8,24–26] but how to estimate the critical or maximum draw ratio precisely before the actual spinning is the next crucial issue.[23]

Although we realize the difficulty of expressing mechanical properties and crystallization with one single index, the correlation between the crystallinity and index *S* is still discussed to illustrate the possible application of the spinning index. In Figure 14, we see the trend of moderately increasing crystallinity with increasing *S* for the three points on the left; the crystallinity then decreases and thereafter increases with *S*. These results show that the influence of the solvent content in the bath may be stronger than the viscosity of the spinning dope on the crystallinity. The proof is that the crystallinity increases sensitively with increasing *S* for the three points on the right. Even though the current index *S* reflects mechanical properties well, it still needs further refinement to predict the crystallization behavior, which is influenced by the viscosity, thermodynamic affinity, and draw ratio.

Although there is room to improve the specific form of index *S*, the possibility of estimating the fiber properties is illustrated. Through index *S*, the estimation of the weighting of each spinning parameter becomes possible. To improve the current index, we have initiated further discussions about the interactions of the spinning parameters (e.g., the relation between the viscosity and the critical draw ratio). In addition, the current index was verified by the PAN precursor fiber, and the concept is applicable to a spinning dope with different polymer types.

CONCLUSIONS

In this study, an existing index of fiber porosity was further developed to reflect the mechanical properties of PAN precursor fibers. At the same time, PAN fibers with different spinning parameters were spun to verify the capability of the current spinning index. The constructions of the spinning index and the observations from experimental results are summarized below:

- A quantitative index S of the spinning process for a polymer/solvent/non-solvent system was proposed to estimate the mechanical properties of fibers. The correlation between spinning parameters, fiber morphology and mechanical properties were established and validated by PAN precursor fibers.
- The tensile modulus and strength of the PAN precursor fibers increase with increasing draw ratio, solvent content in the bath, and solid content of the spinning dope.
- The crystallinity of the PAN precursor fibers increases with the solvent content in the bath and increases slightly with the draw ratio. Refinement of the current index is needed to reflect the crystalline state of fibers.
- As a useful estimation tool, the current index *S* reflects the tensile modulus and tensile strength well. Further development with extensive spinning parameters of the spinning index is recommended to achieve better accuracy of the quality estimation.

REFERENCES

1. Frank, E.; Hermanutz, F.; Buchmeiser, M. R. *Macromol. Mater. Eng.* **2012**, *297*, 493.
2. Donnet, J. B.; Rebouillat, S.; Wang, T. K.; Peng, J. Carbon Fibers; CRC Press: New York, **1998**.
3. Hearle, J. W. S. High-performance Fibres; Woodhead Pub.: Cambridge, **2001**.
4. He, F. Carbon Fiber and Graphite Fiber; Chemical Industry Press: Beijing, **2010**.
5. Hou, C.; Qu, R.; Liang, Y.; Wang, C. *J. Appl. Polym. Sci.* **2005**, *96*, 1529.
6. Ying, L.; Hou, C.; Fei, W. *J. Appl. Polym. Sci.* **2006**, *100*, 4447.
7. Arbab, S.; Noorpanah, P.; Mohammadi, N.; Zeinolebadi, A. *Polym. Bull.* **2011**, *66*, 1267.
8. Bajaj, P.; Sreekumar, T. V.; Sen, K. *J. Appl. Polym. Sci.* **2002**, *86*, 773.
9. Peng, G.-Q.; Zhang, X.-H.; Wen, Y.-F.; Yang, Y.-G.; Liu, L. *J. Macromol. Sci. B Phys.* **2008**, *47*, 1130.
10. Zhang, J.; Zhang, Y.; Zhao, J. *Polym. Bull.* **2011**, *67*, 1073.
11. Sreekumar, T. V.; Liu, T.; Min, B. G.; Guo, H.; Kumar, S.; Hauge, R. H.; Smalley, R. E. *Adv. Mater.* **2004**, *16*, 58.
12. Chae, H. G.; Sreekumar, T. V.; Uchida, T.; Kumar, S. *Polymer* **2005**, *46*, 10925.
13. Jain, R.; Minus, M. L.; Chae, H. G.; Kumar, S. *Macromol. Mater. Eng.* **2010**, *295*, 742.
14. Ruaan, R. C.; Chang, T.; Wang, D. M. *J. Polym. Sci. B Polym. Phys.* **1999**, *37*, 1495.
15. Arbab, S.; Noorpanah, P.; Mohammadi, N.; Soleimani, M. *J. Appl. Polym. Sci.* **2008**, *109*, 3461.
16. Hansen, C. M. *J. Paint. Techn.* **1967**, *39*, 505.
17. Qian, B.; Lin, W.; He, J.; Hu, P.; Wu, C. *J. Polym. Eng.* **1995**, *15*, 327.

18. Tsai, J.-S.; Lin, C.-H. *J. Appl. Polym. Sci.* **1991**, *42*, 3045.
19. Barton, A. F. M. CRC Handbook of Solubility Parameters and Other Cohesion Parameters; CRC Press: Boca Raton, Florida, **1991**.
20. Yilmaz, L.; McHugh, A. *J. Appl. Polym. Sci.* **1986**, *31*, 997.
21. Wang, Y. X.; Wang, C. G.; Yu, M. J. *J. Appl. Polym. Sci.* **2007**, *104*, 3723.
22. Zhou, P.; Lu, C.; Shi, J.; Li, K.; He, F.; Zhang, S.; Li, Y. *J. Macromol. Sci. B Phys.* **2011**, *50*, 1215.
23. Kalb, B.; Pennings, A. J. *J. Mater. Sci.* **1980**, *15*, 2584.
24. Gupta, B.; Revagade, N.; Anjum, N.; Atthoff, B.; Hilborn, J. *J. Appl. Polym. Sci.* **2006**, *100*, 1239.
25. Yu, D.-G.; Chou, W.-L.; Yang, M.-C. *Sep. Purif. Technol.* **2006**, *52*, 380.
26. Arbab, S.; Noorpanah, P.; Mohammadi, N.; Zeinolebadi, A. *J. Polym. Res.* **2011**, *18*, 1343.
27. Liao, C.-C.; Wang, C.-C.; Chen, C.-Y.; Lai, W.-J. *Polymer* **2011**, *52*, 2263.
28. Gupta, A. K.; Singhal, R. P. *J. Polym. Sci. Polym. Phys. Ed.* **1983**, *21*, 2243.
29. Bell, J. P.; Dumbleton, J. *Text. Res. J.* **1971**, *41*, 196.
30. Bashir, Z. *J. Polym. Sci. B Polym. Phys.* **1994**, *32*, 1115.